PHYSICAL REVIEW B **77**, 205320 (2008)

Spin-splitting analysis of a two-dimensional electron gas in almost strain-free $In_{0.89}Ga_{0.11}Sb/In_{0.88}Al_{0.12}Sb$ by magnetoresistance measurements

M. Akabori,[1,2,*] V. A. Guzenko,[2] T. Sato,[1,†] Th. Schäpers,[2] T. Suzuki,[1] and S. Yamada[1]
[1]*Center for Nano Materials and Technology (CNMT), Japan Advanced Institute of Science and Technology (JAIST), 1-1 Asahidai, Nomi, Ishikawa 923-1292, Japan*
[2]*Institute of Bio- and Nanosystems (IBN-1) and Centre of Nanoelectronic Systems for Information Technology (CNI), Research Centre Jülich, 52425 Jülich, Germany*

(Received 24 October 2007; revised manuscript received 25 February 2008; published 20 May 2008)

We investigated the spin-splitting in an almost strain-free $In_{0.89}Ga_{0.11}Sb/In_{0.88}Al_{0.12}Sb$ two-dimensional electron gas (2DEG) by magnetoresistance measurements at 1.5 K. A large effective gyromagnetic factor (g factor) $|g^*|=33-34$ was obtained by means of the coincidence method, which assumes an effective mass $m^*=0.021m_0$ at the Fermi energy. In spite of the large g factor and the high mobility ($\mu=9.8\times10^4$ cm^2/V s), a vanishing spin-splitting was also found around $B\sim0.8$ T by analyzing the second derivative of the magnetoresistance. This effect originates from the interplay between the Rashba and Dresselhaus spin-orbit interactions, and we theoretically confirmed the fact that the Dresselhaus spin-splitting energy $\Delta E_{0D}=3.5$ meV was more than twice as large as the Rashba spin-splitting energy $\Delta E_{0R}=1.5$ meV. Moreover, we demonstrated that the theoretical curves of the normalized spin splitting, including the g factor and the spin-orbit interactions, were well fitted to the experimental points with the Dresselhaus spin-orbit interaction. Therefore, we concluded that the Dresselhaus spin-orbit interaction is dominant in our 2DEG in spite of its narrow band gap.

DOI: 10.1103/PhysRevB.77.205320 PACS number(s): 71.70.Ej, 73.61.Ey, 73.63.Hs, 73.43.Qt

I. INTRODUCTION

Recently, investigations of spin-related phenomena in semiconductors have been paid much attention because they are essential to developing semiconductor spintronic devices, e.g., spin field effect transistors (spin-FETs).[1] The channel of spin-FETs requires having a large spin-orbit interaction in order to control the spin-precession motion of channel electrons at high temperatures. Narrow gap semiconductor two-dimensional electron gases (2DEGs) are promising materials for such spintronic device applications because they essentially have a large gyromagnetic factor (g factor), as well as a strong spin-orbit interaction. These quantities have been mainly characterized by means of magnetoresistance measurements.[2–6] The Zeeman spin-splitting energy, as well as the effective g factor, can be estimated from the peak splitting of the magnetoresistance. The strength of the spin-orbit interaction has been estimated from the beating pattern in the magnetoresistance and has been quantified by the spin-orbit coupling parameter and/or the zero-field spin-splitting energy. In particular, III-V narrow gap semiconductor 2DEGs with InAs or an InAs alloy channel were widely investigated and have revealed the dominance of the Rashba spin-orbit interaction,[2–6] which originates from structure inversion asymmetry[7] and can be controlled by external electric fields, i.e., gate electrodes. Furthermore, the other contribution, i.e., Dresselhaus spin-orbit interaction,[8] which originates from bulk inversion asymmetry has also been discussed[9,10] because it plays an important role in spin-FETs as well.[11]

In this paper, we discuss an InGaSb/InAlSb 2DEG grown on a semi-insulating GaAs (001) substrate. The InGaSb conductive channel has a narrower band gap and a smaller effective electron mass than InAs-based 2DEGs. Therefore, it is expected to show strong spin-related phenomena such as a large Rashba spin-orbit interaction. In similar InSb/InAlSb 2DEGs, high mobility[12] and high frequency operation[13] were already demonstrated. Moreover, evidence of the Rashba spin-orbit interaction,[14] as well as its theoretical support,[15] was reported. However, these heterostructures had a strained InSb channel with respect to the InAlSb barrier layers; thus, it cannot be excluded that the strain introduces a spin-orbit interaction similar to the Rashba one.[4,16,17] A main feature of our 2DEG is an almost strain-free InGaSb channel to the InAlSb barrier layers; thus, it is more suitable to analyze spin-related physical properties in the strain-free channels.

II. EXPERIMENT

Figure 1 shows a schematic layer structure of our InGaSb/InAlSb 2DEG. We grew the 2DEG on a semi-insulating GaAs (001) substrate by using conventional molecular beam epitaxy (MBE) with a Sb cracker cell. The indium contents for the InGaSb and the InAlSb were fixed to 0.89 and 0.88, respectively, being lattice matched to each other. First, a 6-μm-thick $In_{0.88}Al_{0.12}Sb$ buffer layer was directly grown on a GaAs surface. The strain due to the lattice mismatch between InAlSb and GaAs was almost relaxed during the buffer layer growth; thus, the InGaSb/InAlSb layer system became metamorphic. After the buffer layer growth, a 30-nm-thick $In_{0.89}Ga_{0.11}Sb$ channel layer and a 50-nm-thick $In_{0.88}Al_{0.12}Sb$ spacer layer were continuously grown. Next, Si delta doping was carried out, and then a 100-nm-thick $In_{0.88}Al_{0.12}Sb$ barrier layer growth was followed by a 10-nm-thick InSb cap layer growth. In metamorphic systems, the threading dislocations occur due to the strain relaxation. Such threading dislocations can be simply reduced by growing a thick buffer layer because of the pair-annihilation

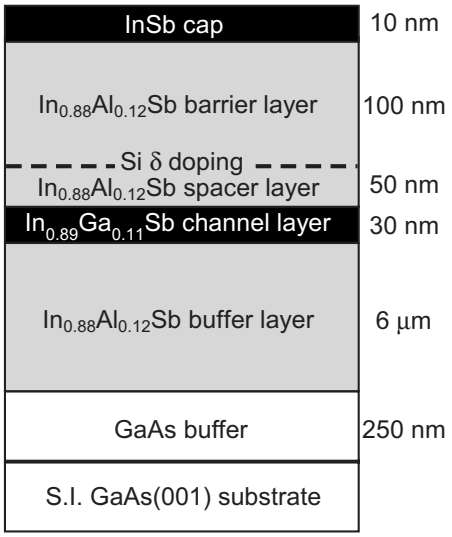

FIG. 1. Schematic layer structure of our InGaSb/InAlSb 2DEG.

mechanism.[18,19] The threading dislocation density near the surface of our 2DEG was estimated to be about 3×10^8 cm^{-2} by plane-view transmission electron microscopy.[20] Moreover, the threading dislocations in the $In_{0.89}Ga_{0.11}Sb$ channel seemed to act as donors; therefore, they also provide channel electrons, whose concentration was estimated to be 1×10^{16} cm^{-3}.[20] Additionally, the dislocations seemed to limit the mobility of the channel electrons due to the ionized scattering.[20]

In order to investigate the transport properties of our 2DEG, we carried out magnetoresistance measurements on Hall-bar structures. The Hall bars were defined by using conventional photolithography techniques. The conductive channel defined by using wet chemical etching was aligned along the [010] direction. The Ohmic contacts were formed by using AuGeNi evaporation and annealing in an Ar/H_2 atmosphere at 250 °C. The channel width and the probe distance were 50 and 200 μm, respectively. The temperature for the magnetoresistance measurements was 1.5 K in a liquid He cryostat with a superconducting magnet. In order to rotate the magnetic field with respect to the plane of the 2DEG, the sample holder was equipped with a tilting mechanism. We used an ac lock-in setup with a typical current of 100 nA for the magnetoresistance measurements. The sheet electron concentration and mobility from the Hall measurement were estimated to be $N_S = 2.9 \times 10^{11}$ cm^{-2} and $\mu = 9.8 \times 10^4$ cm^2/V s, respectively.

III. RESULTS AND DISCUSSION

A. Effective *g* factor

In order to estimate the effective g factor, which determines the Zeeman spin splitting, we applied the coincidence method in the magnetoresistance measurements.[21] Figure 2 shows the magnetoresistance curves for various tilt angles as a function of the inverse magnetic field $1/B_P = 1/(B \cos\theta)$, i.e., the perpendicular component.[22] Shubnikov–de Haas

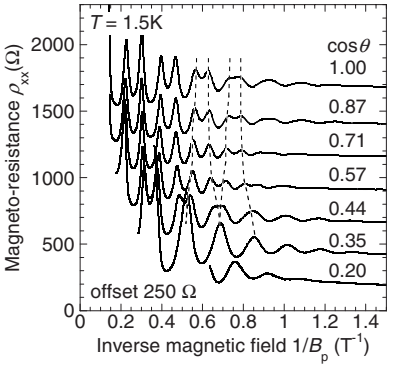

FIG. 2. Magnetoresistance curves as a function of the inverse perpendicular magnetic field $1/B_P$ for various tilted angles. The curves are offset by 250 Ω. The dashed curves are a guide to the eyes to indicate the Zeeman spin-splitting enhancement.

(SdH) oscillations were clearly observed at all angles. With increasing tilt angle θ, each peak splitting of SdH oscillations becomes larger due to the increase in the lateral component in the magnetic field, which corresponds to an increase in the Zeeman spin-splitting. The ratio between the Landau level separation and the Zeeman spin-splitting is an essential parameter in the coincidence method, and it is given by

$$r = \frac{|g^*|\mu_B B}{\hbar\omega_C}, \tag{1}$$

where $|g^*|$ is the absolute value of the effective g factor, $\omega_C = eB_p/m^*$ is the cyclotron frequency, and $\mu_B = \hbar e/2m_0$ is the Bohr magneton. If we define the parameter $\nu = g^* m^*/2m_0$, which is proportional to the product of g^* and m^*, we obtain the following relation:

$$|\nu| = r \cos\theta. \tag{2}$$

By means of the coincidence method, it is possible to experimentally know $|\nu|$. A double frequency of SdH oscillations corresponds to an equidistant separation between the spin-resolved Landau levels, i.e., $r = 1/2$, from Eq. (1). The double frequency was clearly observed at $\cos\theta = 0.71$ ($\theta \approx 45°$); thus, we obtained $|\nu| = 0.36$. A further increase in the tilt angle θ leads to a stronger Zeeman spin-splitting and a phase inverse of the SdH oscillation without the peak splitting corresponds to the coincidence of the spin-up and spin-down levels originating from the neighboring Landau levels, i.e., $r = 1$, from Eq. (1). The phase inverse was observed at $\cos\theta = 0.35$ ($\theta \approx 70°$), which directly resulted in $|\nu| = 0.35$.

Theoretically, the effective g factor is given by[23]

$$g^*_{\text{bulk}} = 2 - \frac{2}{3}\frac{E_P \Delta_{\text{SO}}}{E_G(E_G + \Delta_{\text{SO}})}, \tag{3}$$

where E_G is the band gap energy, Δ_{SO} is the spin-orbit splitting energy, and E_P is the equivalent energy of the interband momentum matrix element. With $E_G = 0.26$ eV, $\Delta_{\text{SO}} = 0.80$ eV, and $E_P = 24$ eV of $In_{0.89}Ga_{0.11}Sb$,[24] the effective g factor is estimated to be −44. This is the value at the conduction band bottom, i.e., the bulk one. With $m^*_{\text{bulk}} = 0.016m_0$, which is the effective mass at the conduction

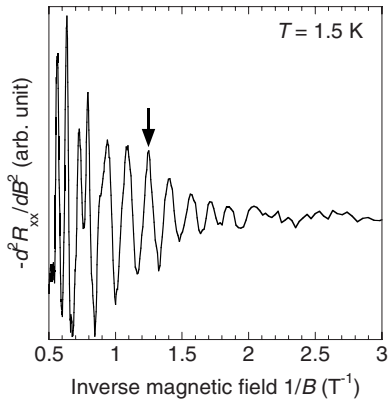

FIG. 3. Second derivative of a magnetoresistance curve as a function of the inverse magnetic field $1/B$. The arrow indicates the narrowest peak corresponding to zero spin splitting.

band bottom, i.e., the bulk value of $In_{0.89}Ga_{0.11}Sb$,[24] we obtain $|\nu|=0.35$, which agrees well with the experimental results.

An absolute value of the effective g factor can be determined from the measured $|\nu|$ value with an effective mass of the electrons at the Fermi energy. By taking nonparabolicity into account, the energy dependence of the effective mass in a narrow gap semiconductor can be calculated from[25]

$$m^* = m^*_{\text{bulk}}\left(1 + \frac{2E}{E_G}\right). \tag{4}$$

Since the 2DEG density of states is also affected by m^*, the Fermi energy of the 2DEG has to be described as follows:

$$E_F = \sqrt{\frac{E_G^2}{4} + \frac{\pi\hbar^2}{m^*_{\text{bulk}}}N_S E_G} - \frac{E_G}{2}. \tag{5}$$

With $E_G=0.26$ eV, $m^*_{\text{bulk}}=0.016m_0$, and $N_S=2.9\times10^{11}$ cm^{-2}, we obtain $E_F=38$ meV. Applying this value into Eq. (4), we obtained $m^*=0.021m_0$ at E_F, which is close to the experimental value of m^* extracted from the cyclotron resonance in our 2DEG.[26] Taking $|\nu|\approx0.35-0.36$ into account, we have determined the absolute value of the effective g factor $|g^*|\approx33-34$.

B. Zero-field spin splitting

In order to investigate zero-field spin-splitting, we analyzed the magnetoresistance curves at low magnetic fields. Figure 3 shows the second derivative of a magnetoresistance curve. The tilt angle θ was 0°, i.e., with the magnetic field B perpendicular to the 2DEG plane and with no lateral component. Clear SdH oscillations with peak splitting were observed at high magnetic fields $1/B<1$ T^{-1} ($B>1$ T); however, one can see that such splitting abruptly vanishes around $1/B\sim1.25$ T^{-1} ($B\sim0.8$ T). At lower magnetic fields $1/B>1.5$ T^{-1} ($B<0.67$ T), the peaks become broad with shoulders and then a beatlike pattern can also be seen. The peak splitting of SdH oscillations generally corresponds to spin-splitting, and the broadening and the beatlike pattern also imply that the spin-splitting appears again at lower magnetic fields. The vanishing of peak splitting means that the spin-splitting energy is close to zero; thus, the spin-splitting effectively vanishes there[22,27] despite the fact that the Landau level broadening of our 2DEG extracted from the cyclotron resonance[26] was sufficiently narrow ($\Gamma\sim0.6$ meV) to show spin splitting at this large g factor. However, the Landau level broadening could not be properly determined from the SdH oscillations because of the background conduction, as well as the spin-splitting. This is completely different from other reports concluding the Rashba spin-orbit interaction in narrow gap semiconductor systems,[3–7,14,15] wherein the spin-splitting energy is almost constant around the Rashba spin-splitting energy until the Zeeman spin-splitting is dominant. A vanishing behavior of spin-splitting was predicted for the GaAs/AlGaAs systems.[28] It originates from the Dresselhaus spin-orbit interaction, which is usually dominant in wide band gap semiconductors. Figures 4(a) and 4(b) show schematics of the spin-resolved Landau levels from $n-1$ to $n+1$ including the Rashba or Dresselhaus spin-orbit interaction.[4] Here, we neglect the k-cubic term of the Dresselhaus spin-orbit interaction. The spin-resolved Landau levels for the Landau index $n=0,1,2,...$ are described as follows:[2–5]

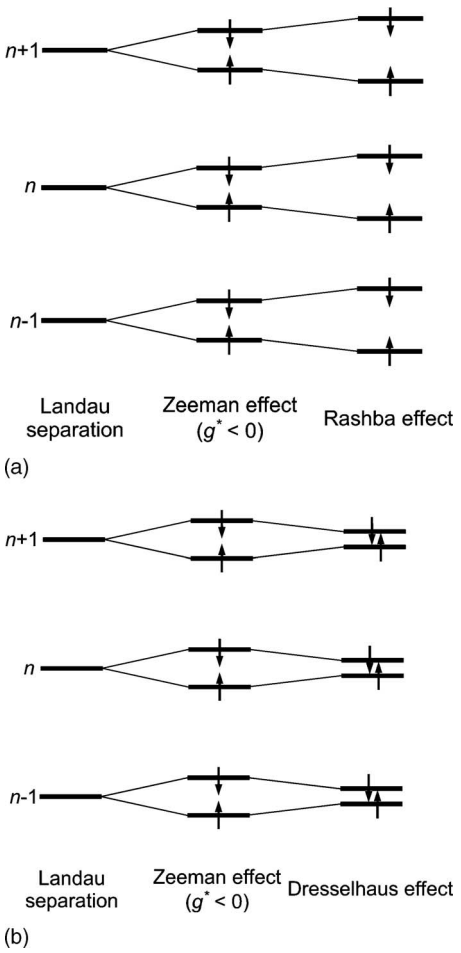

FIG. 4. Schematics of Landau levels (a) with the Rashba spin-orbit interaction and (b) with the Dresselhaus spin-orbit interaction. The effective g factor is negative.

$$E_{n\pm} = \hbar\omega_C \left\{ \left(n + \tfrac{1}{2} \pm \tfrac{1}{2}\right) \mp \tfrac{1}{2}\sqrt{(1-\nu)^2 + \frac{\left(n + \tfrac{1}{2} \pm \tfrac{1}{2}\right)\Delta E_{0R}^2}{E_F \hbar\omega_C}} \right\}, \quad (6)$$

which represents the spin-resolved Landau levels with only the Rashba term, and

$$E_{n\pm} = \hbar\omega_C \left\{ \left(n + \tfrac{1}{2} \mp \tfrac{1}{2}\right) \pm \tfrac{1}{2}\sqrt{(1+\nu)^2 + \frac{\left(n + \tfrac{1}{2} \mp \tfrac{1}{2}\right)\Delta E_{0D}^2}{E_F \hbar\omega_C}} \right\}, \quad (7)$$

which represents the spin-resolved Landau levels with only the Dresselhaus term, where ΔE_{0R} and ΔE_{0D} are the Rashba and Dresselhaus spin-splitting energies, respectively. The Rashba spin-orbit interaction shifts spin-down sublevels E_{n-} upward and spin-up sublevels E_{n+} downward, whereas the Dresselhaus spin-orbit interaction has an opposite effect. When the g factor has a negative value at a large magnetic field, the spin-splitting is enhanced by the Rashba spin-orbit interaction and is suppressed by the Dresselhaus one, as shown in the right sides of Figs. 4(a) and 4(b). As the magnetic field becomes smaller, the influence of the Rashba or Dresselhaus spin-orbit interaction becomes larger compared to that of the Landau separation, as well as the Zeeman spin-splitting, which are both proportional to the magnetic field. In case of the Rashba spin-orbit interaction, the enhancement of spin splitting leads to equidistance between the spin-resolved Landau levels corresponding to a node of the beating of the SdH oscillations. Upon a further decrease in the magnetic field, the enhancement leads to an overlap of neighboring levels with different Landau indices corresponding to an antinode of beating and then, almost periodically, the beating is repeated. In the case of the Dresselhaus spin-orbit interaction, the suppression results in a vanishing spin splitting at a finite magnetic field, as shown by an arrow in Fig. 3, which also corresponds to an antinode of beating. Upon a further decrease in the magnetic field, the spin splitting reappears; however, it has the opposite sign to the Zeeman splitting with the negative g factor, and nodes and antinodes of the SdH oscillation beating appear similar to the Rashba case with a decreasing magnetic field. It indicates that an observation of the SdH beating is not unambiguous evidence of the Rashba spin-orbit interaction.

In order to confirm the dominance of the Dresselhaus spin-orbit interaction, we theoretically estimated the Rashba and the Dresselhaus spin-splitting energies from the calculated conduction band profile. Figure 5 shows the conduction band profile, as well as the distribution of electrons near the channel. The calculation was performed by using a one-dimensional Poisson–Schrödinger solver assuming a surface barrier of 115 meV and a flat band condition at the substrate side. The activated donors are located in the delta doping and the channel regions with the densities of $N_{DD}=1.5\times10^{12}$ cm^{-2} and $N_{CD}=1\times10^{16}$ cm^{-3}, respectively. For this calculation, we did not use the effective mass at the Fermi energy but rather the average effective mass $m^*=0.018m_0$. This value was chosen to satisfy the relation

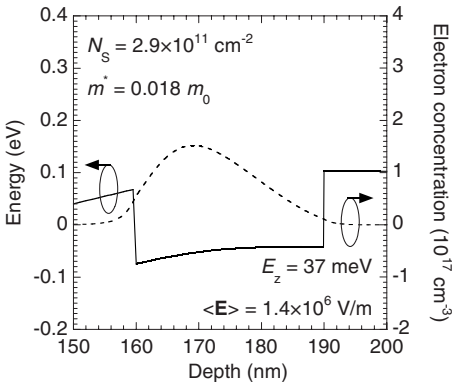

FIG. 5. Calculated conduction band profile (solid curve), as well as the distribution of electron concentration (dashed curve) near the channel.

$$E_F = \frac{\pi\hbar^2}{m^*} N_S, \quad (8)$$

with $N_S=2.9\times10^{11}$ cm^{-2} and $E_F=38$ meV. Furthermore, we obtained the quantum confinement energy $E_z=37$ meV for the ground state level from the conduction band bottom and the average electric field in the channel $\langle E\rangle=1.4\times10^6$ V/m. Since our channel is rather broad (30 nm), we neglected the contributions of the interface and barrier layers to the average electric field $\langle E\rangle$. The Rashba and the Dresselhaus spin-splitting energies can be estimated with these parameters and the weight factors a_{46} and a_{42}.[4] The Rashba and the Dresselhaus spin-orbit coupling parameters are given by

$$a = a_{46}\langle E\rangle, \quad (9)$$

$$\beta = a_{42}\langle k_z^2\rangle, \quad (10)$$

where k_z is z component of wave vector estimated from E_z.[4] The corresponding zero-field spin-splitting energies are given by

$$\Delta E_{0R} = 2ak_F, \quad (11)$$

$$\Delta E_{0D} = 2\beta k_F, \quad (12)$$

where k_F is the Fermi wave vector estimated from E_F.[4] k_z and k_F have almost the same value at present and are estimated to be 1.3×10^8 m^{-1}. We note that the k-cubic term of the Dresselhaus spin-orbit interaction is neglected at present. With $a_{46}=400$ eÅ^2 and $a_{42}=770$ eV Å^3 of InSb,[28] α and β are calculated to be 5.6×10^{-12} eVm and 1.3×10^{-11} eVm, while ΔE_{0R} and ΔE_{0D} are estimated to be 1.5 and 3.5 meV, respectively. Thus, the Dresselhaus spin-splitting energy is more than twice as large as the Rashba spin-splitting energy. As we will show below, the dominance of the Dresselhaus spin-orbit interaction is qualitatively consistent with the experimental result despite the fact that our 2DEG has a narrow band gap channel. The large Dresselhaus contribution in our InSb-based heterostructure mainly results from the large weight factor a_{42} compared to the other material systems. Additionally, the sheet electron concentration of our 2DEG was relatively low; thus, the average electric field was not efficiently large to enhance the Rashba spin-orbit interaction.

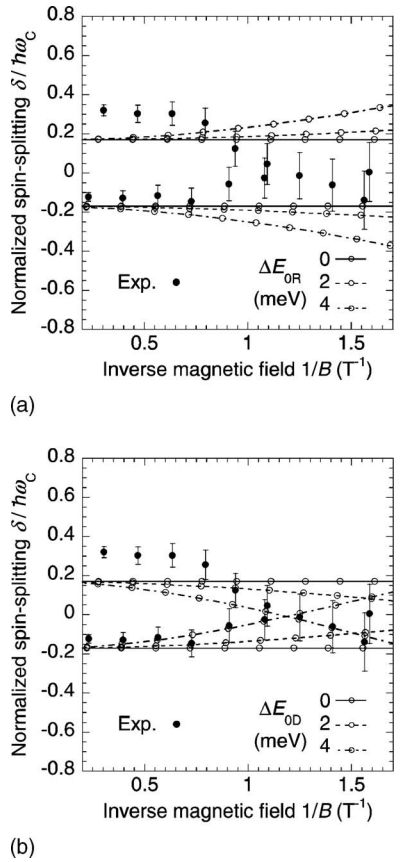

FIG. 6. Magnetic field dependence of the normalized spin splitting with the experimental and the calculated results assuming (a) the Rashba term and (b) the Dresselhaus term. The closed and open circles indicate the experimental and the calculated points, respectively. The error bars of the experimental points correspond to the Landau level broadening of 0.6 meV.

C. Magnetic field dependence of spin-splitting

In order to investigate the spin-splitting behavior in more detail, we compared the experimental result to the theoretical calculations of the magnetic field dependence of normalized spin splitting. We solved Eqs. (6) and (7) for the harmonic energy $\hbar\omega_C$ with the condition of $E_{n\pm}=E_F$, then we defined normalized spin-splitting $\delta/\hbar\omega_C$ as follows:

$$\frac{\delta}{\hbar\omega_C}=\frac{E_{n\pm}}{\hbar\omega_C}-\left(n+\frac{1}{2}\right), \tag{13}$$

where δ implies the additional energy induced by the spin-splitting relative to the spin-degenerated Landau level $\hbar\omega_C(n+1/2)$. In Figs. 6(a) and 6(b), the small open circles with lines as guide to the eyes represent the calculated data from Eqs. (6) and (7). The experimental points taken from Fig. 3 are shown as the large closed circles, assuming $E_F=38$ meV, $m^*=0.018m_0$, and $\nu=-0.35$. In Fig. 6(a), it can be seen that by assuming the Rashba spin-orbit interaction, the spin-splitting monotonously increases with increasing B^{-1}, which is not consistent with the experimental situation. In contrast to Fig. 6(b), i.e., with the Dresselhaus term, the crossing of curves can be confirmed. The crossing point shifts to a higher magnetic field when ΔE_{0D} becomes larger. The crossing corresponds to a vanishing spin-splitting because the Zeeman and Dresselhaus effects cancel each other [cf. Fig. 4(b)]; thus, spin-up and spin-down states are located at the same level. The experimental points around the crossing seem to fit well to $\Delta E_{0D}\sim 4$ meV, which is close to $\Delta E_{0D}=3.5$ meV estimated from the calculated conduction band profile. Additionally, one can see that the spin-up states at a high magnetic field connect to the spin-down states at a low magnetic field and vice versa. It means that the spin-splitting energy at a high magnetic field has the opposite sign of the zero-field spin-splitting energy, as mentioned before. That is completely different from the analysis for the InSb/InAlSb systems of Pfeffer and Zawadzki,[15] which was exclusively based on the Rashba spin-orbit interaction but similar to the prediction for the GaAs/AlGaAs systems of Lommer *et al.*,[28] which was based on the Dresselhaus spin-orbit interaction. Due to the fact that InSb-based materials have an essentially large Dresselhaus spin-orbit interaction and our 2DEG is almost strain-free, i.e., strain-induced effects are negligible, we were able to successfully observe a vanishing spin-splitting and inversion of a sign of the Zeemanlike spin-splitting.

A close inspection of Fig. 6(b) reveals a difference between the experimental points and the calculated curves at a higher magnetic field. This might originate from the exchange interaction among spin-up and spin-down electrons,[29] i.e., due to the difference between spin-up and spin-down electron densities. Since the difference is almost one-half the value of the Landau degeneracy $eB/2h$ and is proportional to B, the exchange interaction gives a constant shift of the normalized spin-splitting at high magnetic fields.

In addition, we have also investigated weak antilocalization in our 2DEG.[30] Weak antilocalization measurements are also an important method to analyze spin-orbit interactions.[31] In our weak antilocalization results, we obtained a zero-field spin-splitting of about 1 meV by fitting the experimental data to a theoretical model of Golub.[32] This value is not consistent with the results obtained by analyzing the SdH oscillations. In order to consistently understand the whole behavior, it is necessary to investigate the magnetoresistance in a wide range of electron concentrations by using a gate electrode, especially from the vanishing field to the zero field, as well as to improve the applicable theoretical models.

IV. CONCLUSION

In conclusion, we investigated the magnetoresistance properties of an almost strain-free $In_{0.89}Ga_{0.11}Sb/In_{0.88}Al_{0.12}Sb$ 2DEG grown on GaAs (001) by MBE. By means of the coincidence method, we extracted a large effective g factor $|g^*|\approx 33-34$ and demonstrated consistency with the theoretically expected value. By analyzing the second derivative of the magnetoresistance, we found that the spin-splitting vanishes around $B\sim 0.8$ T, in spite of the large g factor and the high mobility. We argued that the vanishing spin-splitting originates from the Dresselhaus spin-orbit interaction. In fact, we could theoretically confirm that the

Dresselhaus spin-splitting energy $\Delta E_{0D}=3.5$ meV is larger than the Rashba spin-splitting energy $\Delta E_{0R}=1.5$ meV by calculation based on the conduction band profile of our heterostructure. Moreover, we compared magnetic field dependence of the normalized spin-splitting between the experimental and the theoretical data, and we found good agreement between them at $\Delta E_{0D}\sim 4$ meV. Therefore, we concluded that the Dresselhaus spin-orbit interaction is dominant in our 2DEG in spite of the narrow band gap channel.

ACKNOWLEDGMENTS

The authors thank T. Naito, T. Kakegawa, T. Sunouchi, and T. Harita for their help in the sample fabrication and in the measurements. This work was partially supported by a Grant-in-Aid for Scientific Research in Priority Areas "Semiconductor Nanospintronics" (Contract No. 14076213) of the Ministry of Education, Culture, Sports, Science and Technology, Japan, and also by Mitsubishi and SCAT Foundations for Science and Technology.

*akabori@jaist.ac.jp; m.akabori@fz-juelich.de

†Present address: Advantest Laboratories Ltd. 48-2 Matsubara, Kamiayasi, Aoba, Sendai, Miyagi 989-3124, Japan.

[1] S. Datta and B. Das, Appl. Phys. Lett. **56**, 665 (1990).
[2] J. Luo, H. Munekata, F. F. Fang, and P. J. Stiles, Phys. Rev. B **41**, 7685 (1990).
[3] B. Das, S. Datta, and R. Reifenberger, Phys. Rev. B **41**, 8278 (1990).
[4] J. Nitta, T. Akazaki, H. Takayanagi, and T. Enoki, Phys. Rev. Lett. **78**, 1335 (1997).
[5] Th. Schäpers, G. Engels, J. Lange, Th. Klocke, M. Hollfelder, and H. Lüth, J. Appl. Phys. **83**, 4324 (1998).
[6] Y. Sato, T. Kita, S. Gozu, and S. Yamada, J. Appl. Phys. **89**, 8017 (2001).
[7] Y. A. Bychkov and E. I. Rashba, J. Phys. C **17**, 6039 (1984).
[8] G. Dresselhaus, Phys. Rev. **100**, 580 (1955).
[9] J. B. Miller, D. M. Zumbühl, C. M. Marcus, Y. B. Lyanda-Geller, D. Goldhaber-Gordon, K. Campman, and A. C. Gossard, Phys. Rev. Lett. **90**, 076807 (2003).
[10] S. D. Ganichev, V. V. Bel'kov, L. E. Golub, E. L. Ivchenko, P. Schneider, S. Giglberger, J. Eroms, J. De Boeck, G. Borghs, W. Wegscheider, D. Weiss, and W. Prettl, Phys. Rev. Lett. **92**, 256601 (2004).
[11] J. Schliemann, J. C. Egues, and D. Loss, Phys. Rev. Lett. **90**, 146801 (2003).
[12] K. J. Goldammer, S. J. Chung, W. K. Liu, M. B. Santos, J. L. Hicks, S. Raymond, and S. Q. Murphy, J. Cryst. Growth **201-202**, 753 (1999).
[13] T. Ashley, A. R. Barnes, L. Buckle, S. Datta, A. B. Dean, M. T. Emeny, M. Fearn, D. G. Hayes, K. P. Hilton, R. Jefferies, T. Martin, K. J. Nash, T. J. Phillips, W. H. A. Tang, P. J. Wilding, and R. Chau, Proceedings of the 7th International Conference on Solid-State and Integrated Circuit Technology 2004, edited by R. Huang, M. Yu, J. J. Liou, T. Hiramoto, and C. Claeys (IEEE, 2004), p. 2253.
[14] G. A. Khodaparast, R. E. Doezema, S. J. Chung, K. J. Goldammer, and M. B. Santos, Phys. Rev. B **70**, 155322 (2004).
[15] P. Pfeffer and W. Zawadzki, Phys. Rev. B **68**, 035315 (2003).
[16] S. A. Crooker and D. L. Smith, Phys. Rev. Lett. **94**, 236601 (2005).
[17] D. G. Seiler, B. D. Bajaj, and A. E. Stephens, Phys. Rev. B **16**, 2822 (1977).
[18] J. S. Speck, M. A. Brewer, G. Beltz, A. E. Romanov, and W. Pompe, J. Appl. Phys. **80**, 3808 (1996).
[19] T. Sato, T. Suzuki, S. Tomiya, and S. Yamada, Physica B (Amsterdam) **376-377**, 579 (2006).
[20] T. Sato, Ph.D. thesis, Japan Advanced Institute of Science and Technology, 2006.
[21] J. Nitta, Z. Lin, T. Akayaki, and T. Koga, Appl. Phys. Lett. **83**, 4565 (2003).
[22] M. Akabori, V. A. Guzenko, T. Kakegawa, T. Sato, Th. Schäpers, T. Suzuki, and S. Yamada, Proceedings of the 28th International Conference on the Physics of Semiconductors, AIP Conference Proceedings Vol. 893, edited by W. Jantsch and F. Schaffler (AIP, 2007), p. 1271.
[23] L. M. Roth, B. Lax, and S. Zwerdling, Phys. Rev. **114**, 90 (1959).
[24] I. Vurgaftman, J. R. Meyer, and L. R. Ram-Mohan, J. Appl. Phys. **89**, 5815 (2001).
[25] W. Zawadzki, Adv. Phys. **23**, 435 (1974).
[26] K. Fujii, Y. Hachizawa, and K. Ohnishi, T. Sato, T. Suzuki, S. Yamada, S. Gozu, Proceedings of the 12th International Conference on Narrow Gap Semiconductors, Institute of Physics Conference Series No. 187, edited by J. Kono and J. Léotin (Taylor & Francis, 2006), p. 61.
[27] M. Akabori, T. Sunouchi, T. Kakegawa, T. Sato, T. Suzuki, and S. Yamada, Physica E (Amsterdam) **34**, 413 (2006).
[28] G. Lommer, F. Malcher, and U. Rössler, Phys. Rev. Lett. **60**, 728 (1988).
[29] T. Ando and Y. Uemura, J. Phys. Soc. Jpn. **37**, 1044 (1974).
[30] V. A. Guzenko, M. Akabori, Th. Schäpers, S. Cabañas, T. Sato, T. Suzuki, and S. Yamada, Phys. Status Solidi C **3**, 4227 (2006).
[31] T. Koga, J. Nitta, T. Akazaki, and H. Takayanagi, Phys. Rev. Lett. **89**, 046801 (2002).
[32] L. E. Golub, Phys. Rev. B **71**, 235310 (2005).